Review of diffraction in COMPASS

Fabian Krinner
for the COMPASS collaboration

Physik-Department E18
Technische Universität München

Diffractive and electromagnetic
processes at high energies
Bad Honnef

Content

- The COMPASS experiment
- The two-step fit procedure
  - Step 1: Partial-Wave decomposition
  - Step 2: The mass-dependent fit
- Results
  - The major waves
  - The new $a_1(1420)$ resonance
  - A spin-exotic signal with $J^{PC} = 1^{-+}$
- New Directions
  - Non-isobaric waves
  - Freed-isobar approach
- Conclusions

The COMPASS-experiment

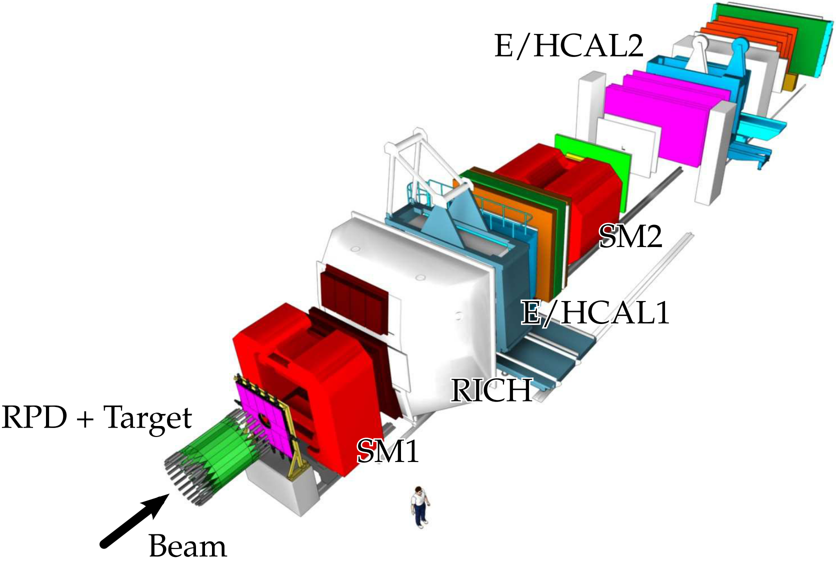
E/HCAL2
SM2
E/HCAL1
RICH
RPD + Target
SM1
Beam

The COMPASS Experiment

- Fixed-target experiment at CERN's northern area
- Various configurations possible:
  - Secondary hadron beams
  - Polarized Tertiary muon beams
  - Various (polarized) targets
- Good acceptance over wide kinematic range
- Particle identification via RICH and CEDARs
- Broad physics program
- Analysis presented here:
  - 190 GeV/c hadron beam, mainly π^-
  - 40 cm liquid hydrogen target

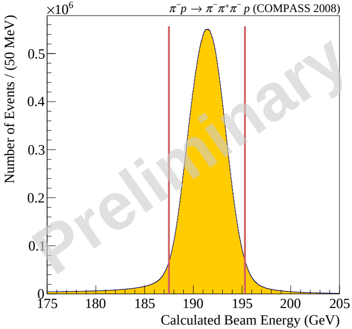

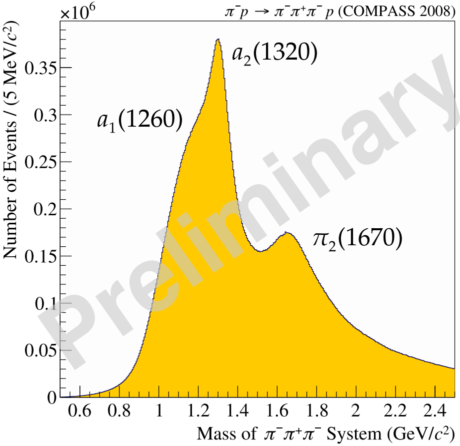

- Channel presented here: $\pi^-_{\text{beam}} p \to \pi^-\pi^+\pi^- p_{\text{recoil}}$

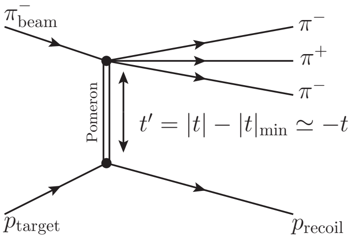

- Around 50 million events recorded
- Up to now largest data-set for this channel

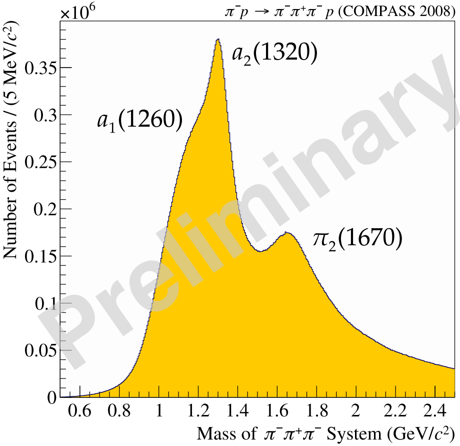

- Channel presented here:
  $\pi^-_{\text{beam}} p \to \pi^-\pi^+\pi^- p_{\text{recoil}}$

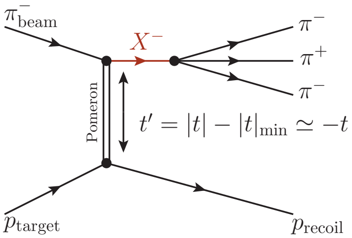

- Around 50 million events recorded
- Up to now largest data-set for this channel
- Structures → intermediate states

The two-step fit procedure

- Goal: Extraction of quantum numbers, masses and widths of these intermediate states
- Two-step procedure:
  - Step 1: Partial-Wave decomposition
  - Step 2: Fit of mass shapes
- Advantages of two steps:
  - Less computational requirements than a global fit
  - No model for resonance shapes necessary in the first step

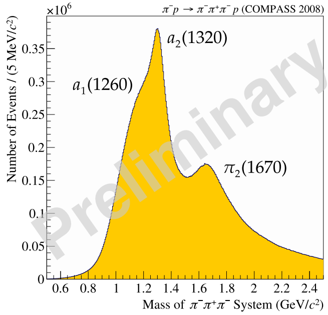

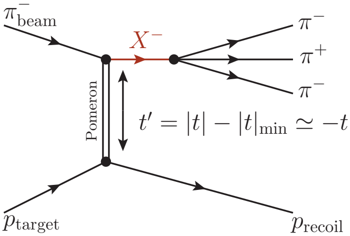

Step 1
Partial-Wave decomposition

- Extended likelihood function: Probability to measure the events given the model
- $\mathcal{L} =$

$$p(N_{\text{observed}}) \prod_{\text{event}}^{N_{\text{observed}}} p(\text{event}) = \underbrace{\frac{N_{\text{expected}}^{N_{\text{observed}}}}{N_{\text{observed}}!} e^{-N_{\text{expected}}}}_{\text{Poisson factor}} \underbrace{\prod_{\text{events}}^{N_{\text{observed}}} \mathcal{I}(\text{event})\eta(\text{event})}_{\text{Probability of single events}}$$

  - Intensity $\mathcal{I} = |\mathcal{A}|^2$ modeled
  - Detection efficiency η of the detector from Monte Carlo
- Write complex amplitude $\mathcal{A}(\text{event})$ as:

$$\mathcal{A}(\text{event}) = \sum_i T_i \mathcal{A}_i(\text{event})$$

- Single amplitudes $\mathcal{A}_i(\text{event})$ known, magnitude and phase, T_i, unknown
- Fit result: Production amplitudes T_i at the maximum of the likelihood

Step 1: Partial-Wave decomposition
The *isobar model*

- Structures in the Dalitz plots at different masses $m_X = m_{3\pi}$
- Additional $\pi^-\pi^+$ intermediate states appear

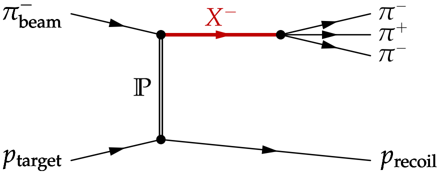

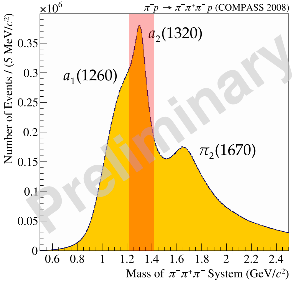

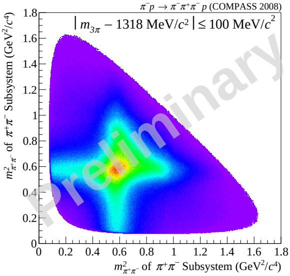

- Structures in the Dalitz plots at different masses $m_X = m_{3\pi}$
- Additional $\pi^-\pi^+$ intermediate states appear

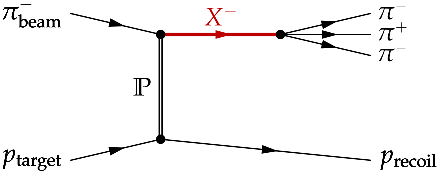

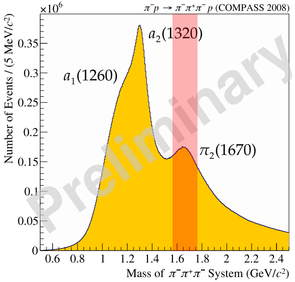

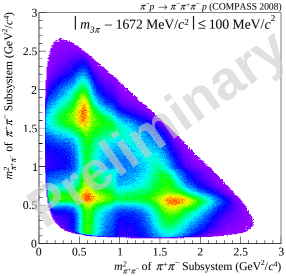

Step 1: Partial-Wave decomposition

The *isobar model*

- Structures in the Dalitz plots at different masses $m_X = m_{3\pi}$
- Additional $\pi^-\pi^+$ intermediate states appear
  $\rightarrow$ Subsequent two-particle decays: *Isobar model*

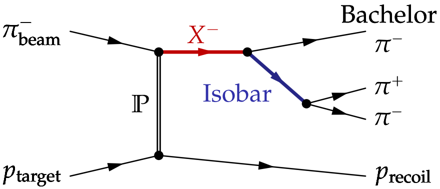

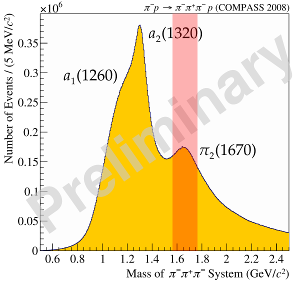

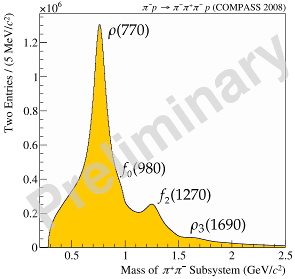

Model the amplitude as a sum over Partial-Waves:

- Expand $\mathcal{A}$ as a series of Partial-Waves

$$\mathcal{A} = \sum_{\text{waves}} T_{\text{wave}} \mathcal{A}_{\text{wave}}$$

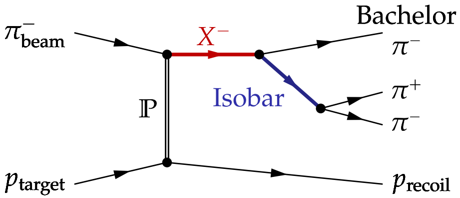

- Wave given by:

  $J^{PC} M^{\epsilon} [\text{isobar}] \pi L$ (e.g. $1^{++}0^{+}\rho(770)\pi S$)

- Examples for isobars:

J^{PC}	Isobars
0^{++}	$f_0(500)$ (or σ or $[\pi\pi]_S$), $f_0(980)$, $f_0(1500)$
1^{--}	$\rho(770)$
2^{++}	$f_2(1270)$
3^{--}	$\rho_3(1690)$

- In principle also excited isobars or higher spins possible

- Amplitude $\mathcal{A} = \sum_{\text{waves}} T_{\text{wave}} \mathcal{A}_{\text{wave}}$
- In principle: Sum over infinite spins and all isobars
- Truncate at some point
- Results may depend on truncation (Example shown later)
- What are the relevant waves for the data-set?

- Amplitude $\mathcal{A} = \sum_{\text{waves}} T_{\text{wave}} \mathcal{A}_{\text{wave}}$
- In principle: Sum over infinite spins and all isobars
- Truncate at some point
- Results may depend on truncation (Example shown later)
- What are the relevant waves for the data-set?
- Now in use: 88 waves

$0^{-+}0^{+} f_0(1500)\pi S$
$0^{-+}0^{+} f_0(980)\pi S$
$0^{-+}0^{+} f_2(1270)\pi D$
$0^{-+}0^{+} \rho(770)\pi P$
$0^{-+}0^{+} \sigma\pi S$

$1^{++}0^{+} f_0(980)\pi P$
$1^{++}0^{+} f_2(1270)\pi P$
$1^{++}0^{+} f_2(1270)\pi F$
$1^{++}0^{+} \rho_3(1690)\pi D$
$1^{++}0^{+} \rho_3(1690)\pi G$
$1^{++}0^{+} \rho(770)\pi S$
$1^{++}0^{+} \rho(770)\pi D$
$1^{++}0^{+} \sigma\pi P$
$1^{++}1^{+} f_0(980)\pi P$
$1^{++}1^{+} f_2(1270)\pi P$
$1^{++}1^{+} \rho(770)\pi S$
$1^{++}1^{+} \rho(770)\pi D$
$1^{++}1^{+} \sigma\pi P$

$1^{-+}1^{+} \rho(770)\pi P$

$2^{++}1^{+} f_2(1270)\pi P$
$2^{++}1^{+} \rho_3(1690)\pi D$
$2^{++}1^{+} \rho(770)\pi D$
$2^{++}2^{+} f_2(1270)\pi P$
$2^{++}2^{+} \rho(770)\pi D$

$2^{-+}0^{+} f_0(980)\pi D$
$2^{-+}0^{+} f_2(1270)\pi S$
$2^{-+}0^{+} f_2(1270)\pi D$
$2^{-+}0^{+} f_2(1270)\pi G$
$2^{-+}0^{+} \rho_3(1690)\pi P$
$2^{-+}0^{+} \rho(770)\pi P$
$2^{-+}0^{+} \rho(770)\pi F$
$2^{-+}0^{+} \sigma\pi D$
$2^{-+}1^{+} f_2(1270)\pi S$
$2^{-+}1^{+} f_2(1270)\pi D$
$2^{-+}1^{+} \rho_3(1690)\pi P$
$2^{-+}1^{+} \rho(770)\pi P$
$2^{-+}1^{+} \rho(770)\pi F$
$2^{-+}1^{+} \sigma\pi D$
$2^{-+}2^{+} f_2(1270)\pi S$
$2^{-+}2^{+} f_2(1270)\pi D$
$2^{-+}2^{+} \rho(770)\pi P$

$3^{++}0^{+} f_2(1270)\pi P$
$3^{++}0^{+} \rho_3(1690)\pi S$
$3^{++}0^{+} \rho_3(1690)\pi 6$
$3^{++}0^{+} \rho(770)\pi D$
$3^{++}0^{+} \rho(770)\pi G$
$3^{++}0^{+} \sigma\pi F$
$3^{++}1^{+} f_2(1270)\pi P$
$3^{++}1^{+} \rho_3(1690)\pi S$
$3^{++}1^{+} \rho(770)\pi D$
$3^{++}1^{+} \rho(770)\pi G$
$3^{++}1^{+} \sigma\pi F$

$3^{-+}1^{+} f_2(1270)\pi D$
$3^{-+}1^{+} \rho(770)\pi F$

$4^{++}1^{+} f_2(1270)\pi F$
$4^{++}1^{+} \rho_3(1690)\pi D$
$4^{++}1^{+} \rho(770)\pi G$
$4^{++}2^{+} f_2(1270)\pi F$
$4^{++}2^{+} \rho(770)\pi G$

$4^{-+}0^{+} f_2(1270)\pi D$
$4^{-+}0^{+} f_2(1270)\pi G$
$4^{-+}0^{+} \rho(770)\pi F$
$4^{-+}0^{+} \sigma\pi G$
$4^{-+}1^{+} f_2(1270)\pi D$
$4^{-+}1^{+} \rho(770)\pi F$

$5^{++}0^{+} f_2(1270)\pi F$
$5^{++}0^{+} f_2(1270)\pi H$
$5^{++}0^{+} \rho_3(1690)\pi D$
$5^{++}0^{+} \rho(770)\pi G$
$5^{++}0^{+} \sigma\pi H$
$5^{++}1^{+} f_2(1270)\pi F$
$5^{++}1^{+} \sigma\pi H$

$6^{++}1^{+} f_2(1270)\pi H$
$6^{++}1^{+} \rho(770)\pi 6$

$6^{-+}0^{+} f_2(1270)\pi G$
$6^{-+}0^{+} \rho_3(1690)\pi F$
$6^{-+}0^{+} \rho(770)\pi H$
$6^{-+}0^{+} \sigma\pi 6$
$6^{-+}1^{+} \rho(770)\pi H$
$6^{-+}1^{+} \sigma\pi 6$

$1^{++}1^{-} \rho(770)\pi S$
$1^{-+}0^{-} \rho(770)\pi P$
$1^{-+}1^{-} \rho(770)\pi P$
$2^{++}0^{-} f_2(1270)\pi P$
$2^{++}0^{-} \rho(770)\pi D$
$2^{++}1^{-} f_2(1270)\pi P$
$2^{-+}1^{-} f_2(1270)\pi S$

- Fit 88 wave model to the data

$$\mathcal{A}(m_{3\pi}, t', \tau) = \sum_{\text{waves}} T_{\text{wave}}(m_{3\pi}, t')\mathcal{A}_{\text{wave}}(\tau)$$

- $m_{3\pi}$ and t' dependence unknown
- Fit independently in bins of mass $m_{3\pi}$ and four-momentum transfer t':
  - 100 bins in $m_{3\pi}$ from $0.5 - 2.5\,\mathrm{GeV}$
  - 11 non-equidistant bins in t'
- 1100 independent fits with up to 175 free parameters
- $m_{3\pi}$-dependence of the results $\rightarrow$ extract resonances

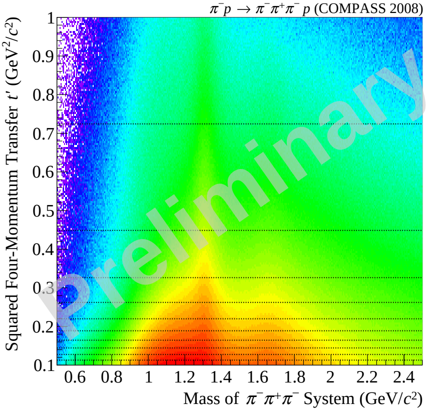

- Two channels:
  $\pi^- p \to \pi^-\pi^+\pi^- p$
  and
  $\pi^- p \to \pi^-\pi^0\pi^0 p$
- Intensity plotted:
  $\mathcal{I} = |T_{\mathrm{wave}}(m_{3\pi})|^2$
- $J^{PC} = 1^{++}$:
  axial-vector
- $\sim$ 33% of the total intensity

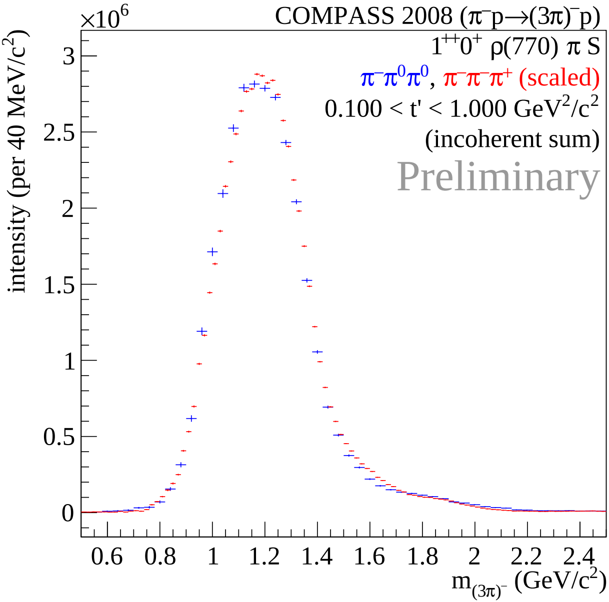

- $J^{PC} = 2^{++}$: tensor
- Clearest resonance
- $\sim$ 8% of the total intensity

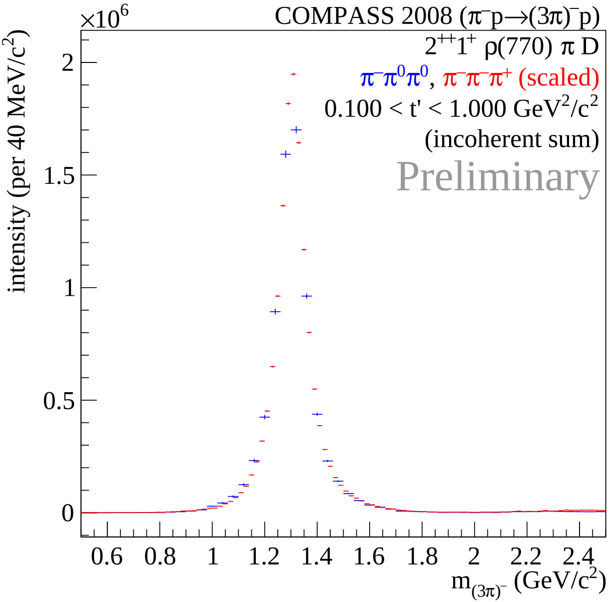

- $J^{PC} = 2^{-+}$: pion with spin 2
- $\sim$ 7% of the total intensity

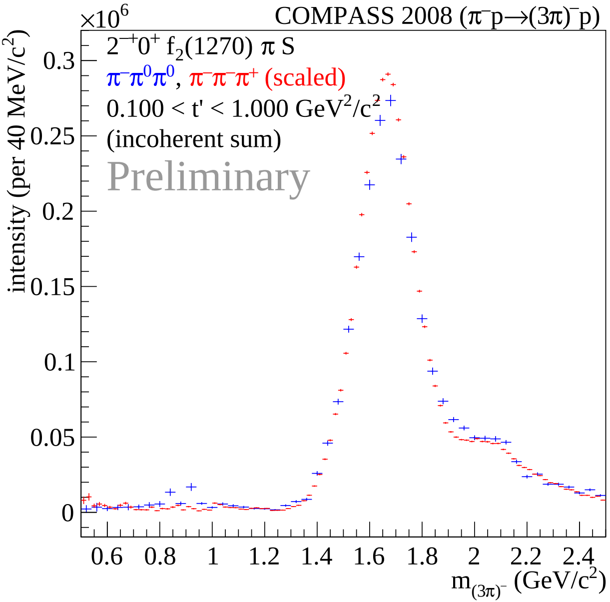

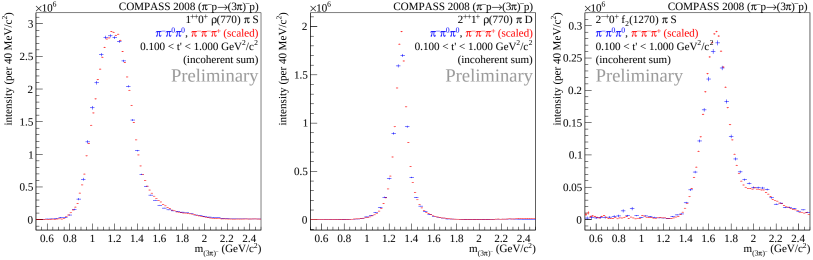

- Main features of the observed spectrum explained by major waves
- Known intermediate states identified
- Good agreement between both channels
- Up to now, resonance parameters not extracted

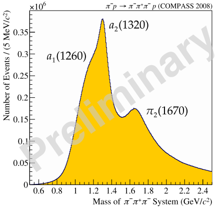

- Spin-4 meson decaying into $\rho(770)\ \pi$
- Only 0.76% of the intensity in the $\pi^-\pi^+\pi^-$ channel
- The well known $a_4(2040)$ resonance is clearly visible
- PWA also allows to clearly extract waves on sub-percent level

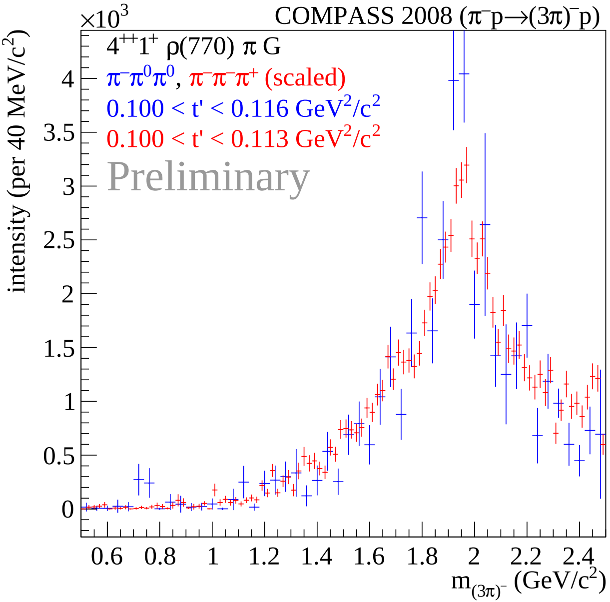

Step2
The mass-dependent fit

- Extract resonance parameters from the results of the first step
- Higher spin waves mostly non-resonant
- $\rightarrow$ Only subset of the waves is modeled in second step
- Relative phases help finding resonances

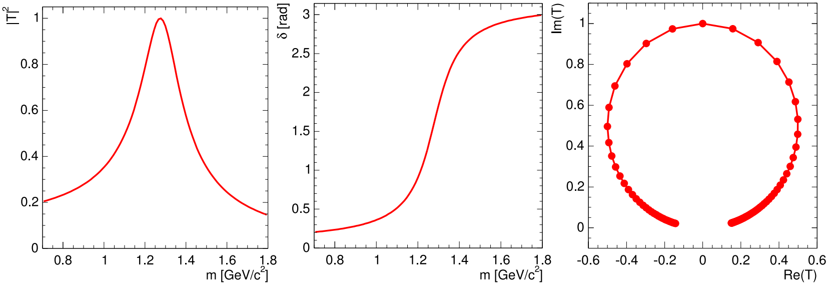

- T_{wave} contain resonant structures

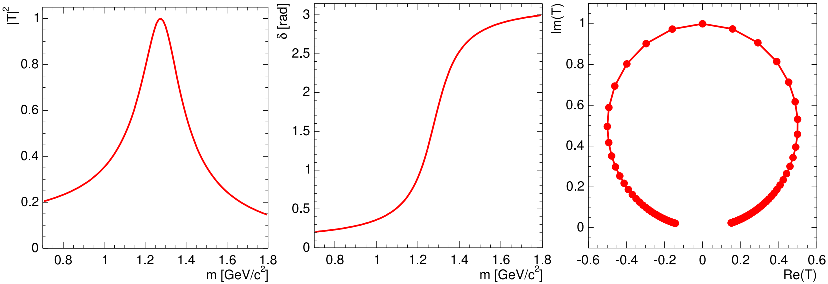

- T_{wave} contain resonant structures
- Resonances:
  - Intensity structure (peak or dip)
  - Phase motion

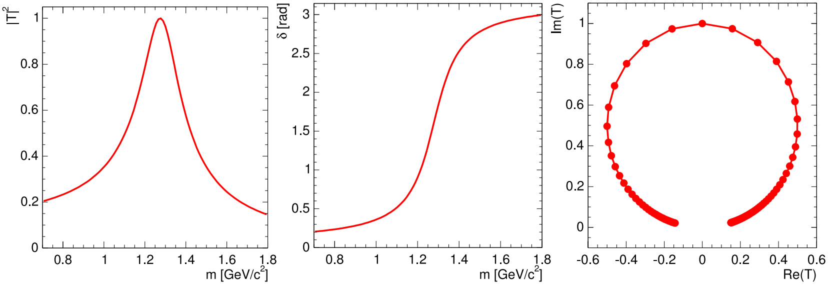

- T_{wave} contain resonant structures
- Resonances:
  - Intensity structure (peak or dip)
  - Phase motion
- Similar to the harmonic oscillator:
  - Intensity: Energy in the oscillator at a certain excitation frequency
  - Phase: Phase between the displacement and the driving force

- Use e.g. Breit-Wigner parametrization:

$$BW(m_{3\pi}) = \frac{m_0\Gamma_0}{m_0^2 - m_{3\pi}^2 - im_0\Gamma_0}$$

- More sophisticated parameterizations possible (e.g. $\Gamma_0 \to \Gamma(m_{3\pi})$)
- Add real-valued non-resonant component $NR(m_{3\pi})$
- Total model for production amplitudes

$$\mathcal{T}_{\text{wave}} = \sum_{\text{resonances}} C_i BW_i(m_{3\pi}) + C_{NR} NR(m_{3\pi})$$

- Complex "coupling parameters" C_i, no direct physical meaning

- Free global phase in every bin
- Do not fit amplitudes, but spin-density matrix

$$\rho_{ij}(m_{3\pi}, t') = T_i(m_{3\pi}, t') T_j^*(m_{3\pi}, t')$$

- Global phase cancels
- Phase helps to identify resonances
- *"Not every peak is a resonance and not every resonance is a peak"*
- Separate matrix for every t' bin

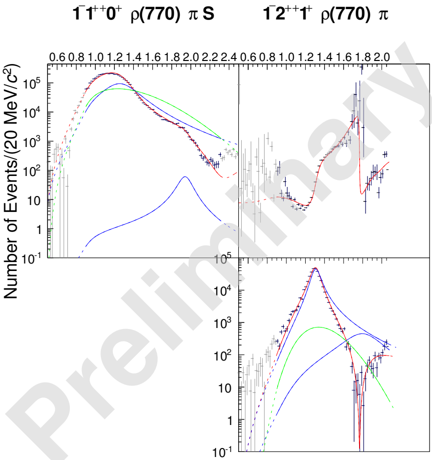

- Free global phase in every bin
- Do not fit amplitudes, but spin-density matrix

$$\rho_{ij}(m_{3\pi}, t') = T_i(m_{3\pi}, t') T_j^*(m_{3\pi}, t')$$

- Global phase cancels
- Phase helps to identify resonances
- *“Not every peak is a resonance and not every resonance is a peak”*
- Separate matrix for every t' bin

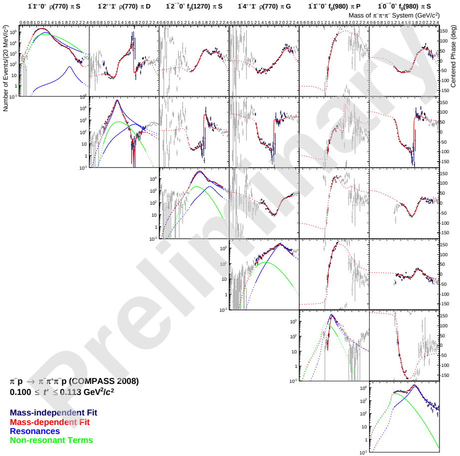

- Construct $\chi^2(\vec{\theta})$ function:

$$\chi^2(\vec{\theta}) = \sum_{\text{bins}} \sum_{i,j} \left(\frac{\rho_{ij}(m_{3\pi}, t') - \mathcal{T}_i(m_{3\pi}, t'; \vec{\theta}) \mathcal{T}_j^*(m_{3\pi}, t'; \vec{\theta})}{\Delta\rho_{ij}(m_{3\pi}, t')} \right)^2$$

- Vector of fit parameters $\vec{\theta}$
- Serveral hundred free parameters
- Two types:
  - "Complex couplings" C_i free in every bin of the four-momentum transfer t'
  - Parameters of interest: m_0, Γ_0 of the resonances (only 10%)
- Result: Parameters at minimum of χ^2

- Many possible parameterizations for resonant and non-resonant contributions
- Results depend on chosen subset of waves
- $\rightarrow$ Model-dependent results

- Lots of parameters with non-linearities
- Many local minima in the χ^2 function
- Results depend on start-values for the minimization of χ^2
- $\rightarrow$ Many fit attempts necessary (> 1000)

- $\rightarrow$ Extensive systematic studies

Step 2: The mass-dependent fit

Fit result

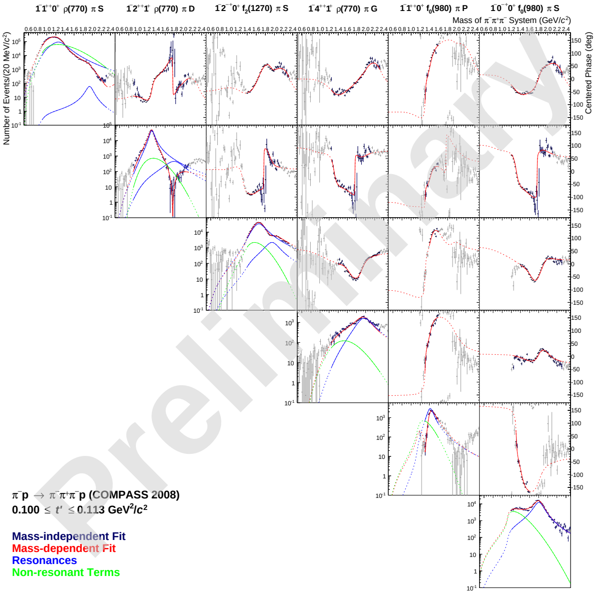

- Fit with six waves
- Five different sets of quantum numbers
- Eleven t' bins in total
- Shape parameters the same in all bins of t'
- Complex couplings vary with t'
- Better separation between resonant and non-resonant contributions

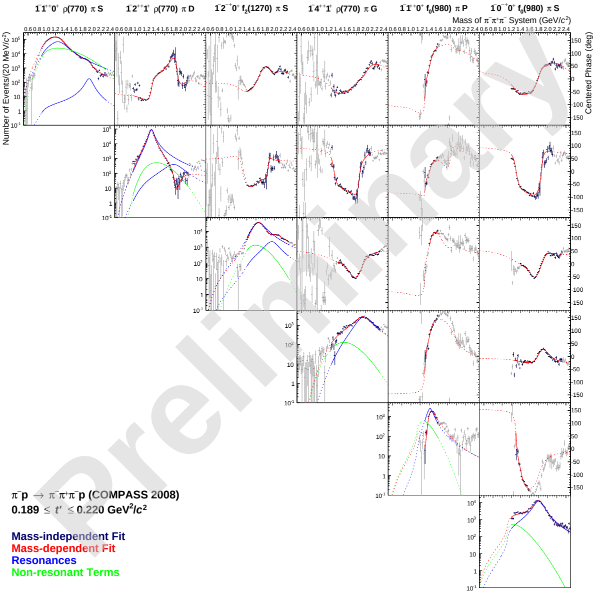

- Fit with six waves
- Five different sets of quantum numbers
- Eleven t' bins in total
- Shape parameters the same in all bins of t'
- Complex couplings vary with t'
- Better separation between resonant and non-resonant contributions

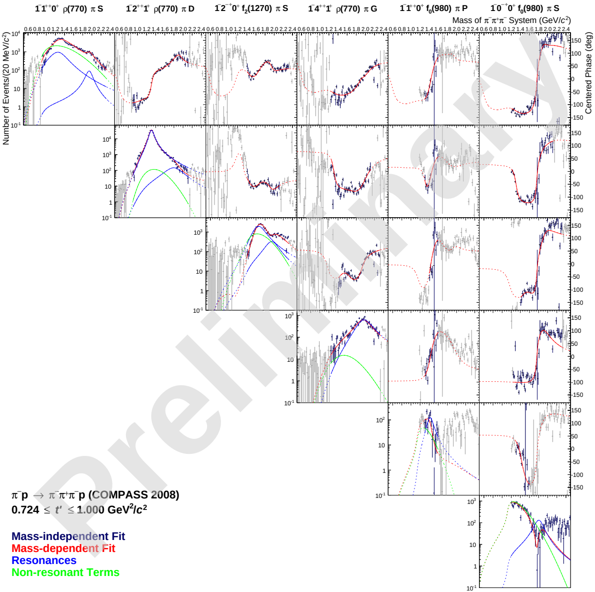

- Fit with six waves
- Five different sets of quantum numbers
- Eleven t' bins in total
- Shape parameters the same in all bins of t'
- Complex couplings vary with t'
- Better separation between resonant and non-resonant contributions

The major waves

- Main resonance: $a_2(1320)$
- Peak position stable
- Nearly no non-resonant contributions
- Clearest resonance in the analysis

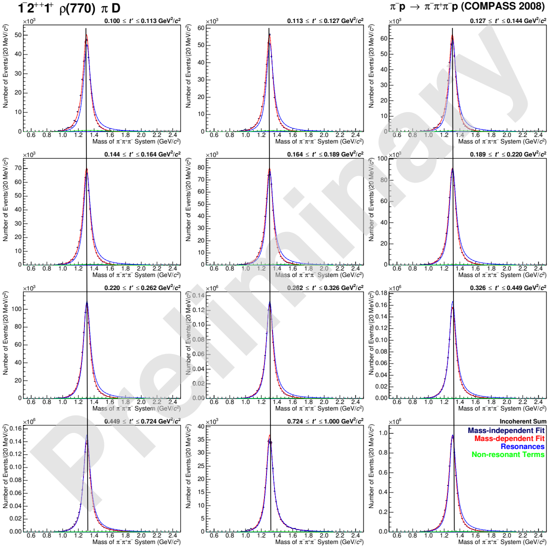

- Main resonance: $a_1(1260)$
- Peak of the intensity moves with t'
- Peak of the resonance fixed with t'
- Binning in the four-momentum transfer allows better differentiation between resonant and non-resonant structures

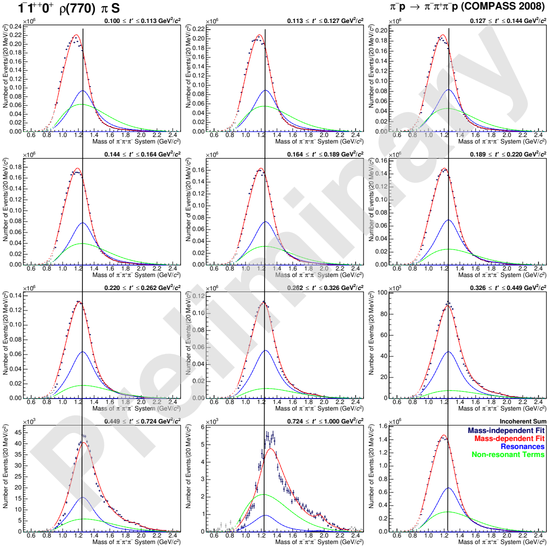

The major waves

- Main resonance $\pi_2(1670)$
- Peak position also stable
- Second resonance appears as shoulder
- Second resonance $\pi_2(1880)$

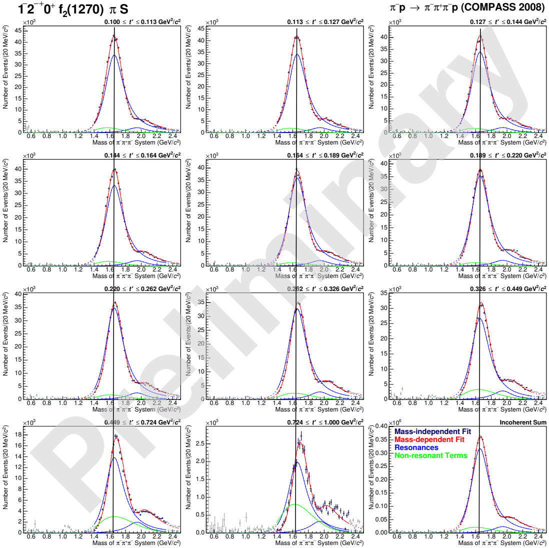

A new resonance
The $a_1(1420)$

- Previously unknown peak observed in

$$1^{++}0^{+} f_0(980)\pi P$$

- Corresponds to a resonance?

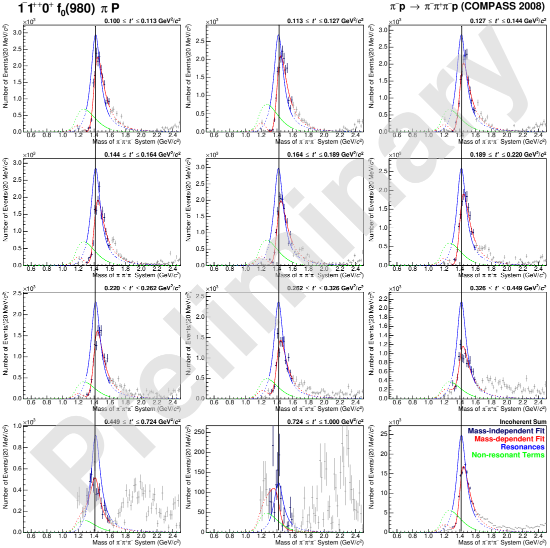

The new $a_1(1420)$ resonance

Peak in intensity and phase motion:

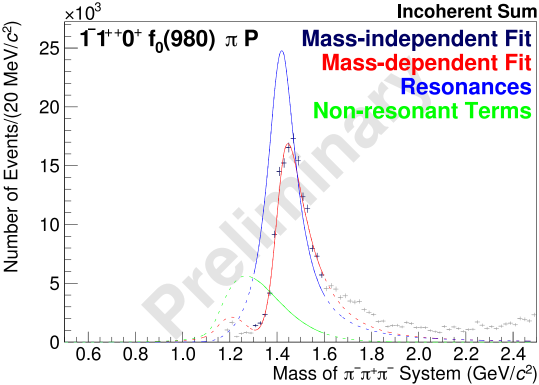

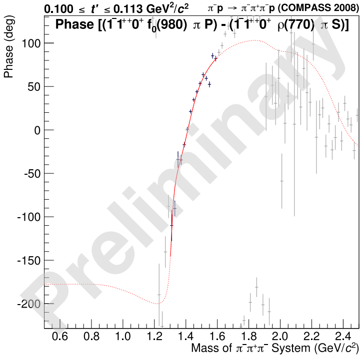

Phase motion w.r.t. other waves → peak corresponds to a resonance

arXiv:1501.05732, to be published in PRL (Editors' choice)

The new $a_1(1420)$ resonance

Peak in intensity and phase motion:

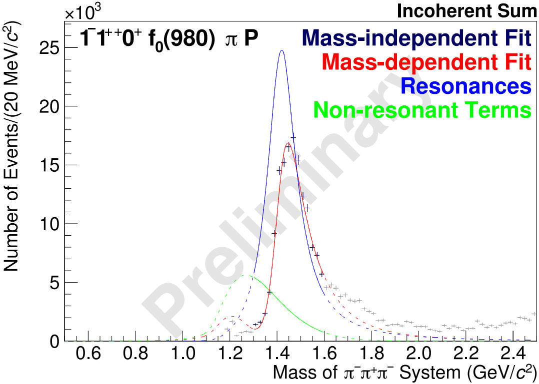

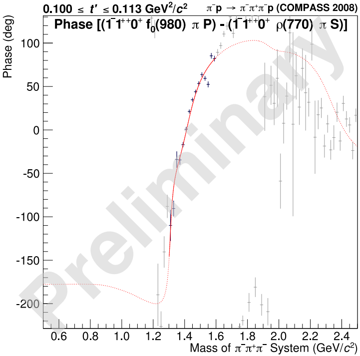

Phase motion w.r.t. other waves → peak corresponds to a resonance

Extracted Breit-Wigner parameters:

$$m_{a_1(1420)} = 1414^{+15}_{-13}\,\mathrm{MeV}/c^2;\ \Gamma_{a_1(1420)} = 152^{+8}_{-23}\,\mathrm{MeV}/c^2$$

arXiv:1501.05732, to be published in PRL (Editors' choice)

- Never observed before
- $J^{PC} = 1^{++}$: axial-vector meson
- New resonance: $a_1(1420)$
- Nature unclear:
  - Not expected in quark-model
  - Special decay
  - Analogue to X, Y, Z states?
  - Dynamically generated?

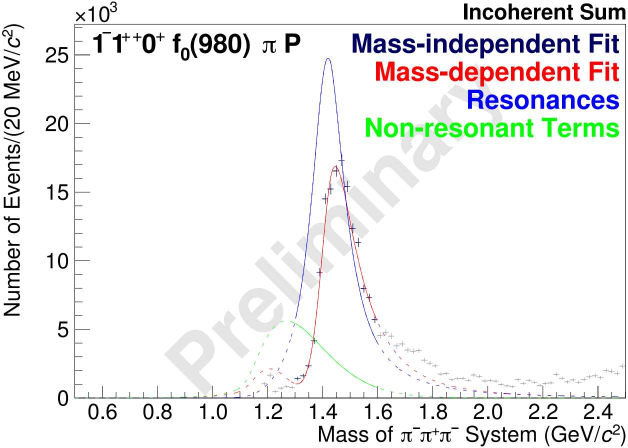

Seel also: [Wang, arXiv:1401.1134], [Chen et al., Phys. Rev. **D91** (2015) 094022], [Basdevant and Berger, Phys. Rev. Lett. **114** (2015) 192001 and arXiv:1501.04643] and [Mikhasenko et al., Phys. Rev. **D91** (2015) 094015]

Spin exotic wave

$\pi_1(\ldots)$

- Quark-antiquark pair
  - Spin couples to: $S = 0, 1$
  - Total meson spin: $\vec{J} = \vec{L} + \vec{S}$
  - Other quantum numbers:
    - Parity: $P = (-1)^{L+1}$
    - Generalized charge conjugation: $C = (-1)^{L+S}$

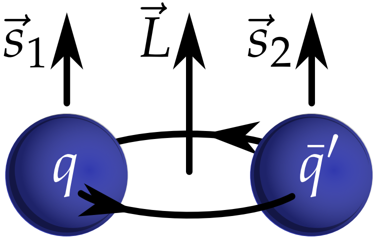

- Quark-antiquark pair
  - Spin couples to: $S = 0, 1$
  - Total meson spin: $\vec{J} = \vec{L} + \vec{S}$
  - Other quantum numbers:
    - Parity: $P = (-1)^{L+1}$
    - Generalized charge conjugation: $C = (-1)^{L+S}$

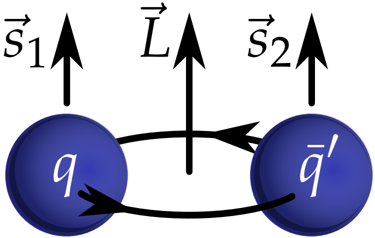

- *Forbidden* combinations exist, e.g.: $J^{PC} = 0^{--}, 0^{+-}, 1^{-+}, 2^{+-}, \ldots$

- Quark-antiquark pair
  - Spin couples to: $S = 0, 1$
  - Total meson spin: $\vec{J} = \vec{L} + \vec{S}$
  - Other quantum numbers:
    - ★ Parity: $P = (-1)^{L+1}$
    - ★ Generalized charge conjugation: $C = (-1)^{L+S}$

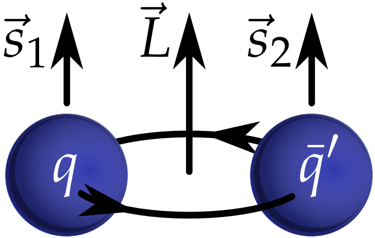

- *Forbidden* combinations exist, e.g.: $J^{PC} = 0^{--}, 0^{+-}, 1^{-+}, 2^{+-}, \ldots$

- Observe forbidden $J^{PC} \rightarrow$ no $q\bar{q}$-state

- Signal with spin exotic quantum numbers
- $J^{PC} = 1^{-+}$: pion with spin 1
- Cannot be explained as $q\bar{q}$-pair
- $\rightarrow$ Has to be something different

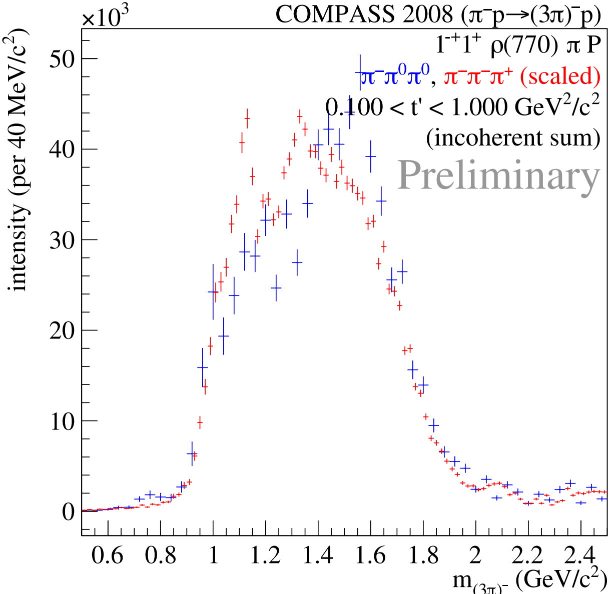

BNL E852

- Same wave also analyzed in different experiments

BNL E852

- Very different results

VES

- Wave-sets for the fits different
- 21, 36, 44 or 42 waves used

COMPASS

- Wave-set selection very important

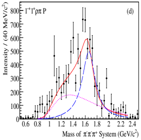

A spin-exotic signal with $J^{PC} = 1^{-+}$

Comparison with *Deck-model* at different t'-bins

- Fit in t' bins allows closer look
- Low t': Broad structure
- High t': Peak remains

$0.100 < t' < 0.113\,(\mathrm{GeV}/c)^2$

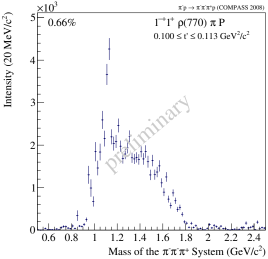

$0.326 < t' < 0.449\,(\mathrm{GeV}/c)^2$

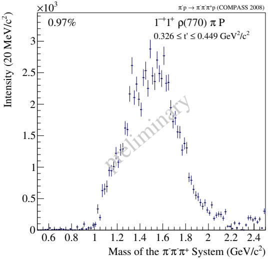

$0.164 < t' < 0.189\,(\mathrm{GeV}/c)^2$

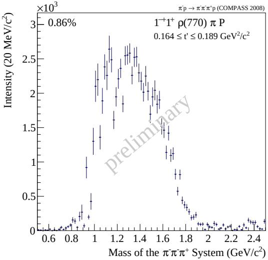

$0.724 < t' < 1.000\,(\mathrm{GeV}/c)^2$

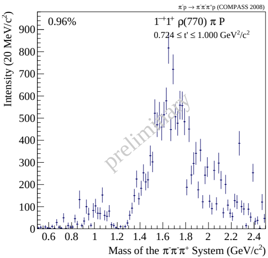

- Signal not necessarily from resonances
- Possible origin: Non-resonant contribution:
  - Same initial and final state
  - No intermediate 3π resonances appear

A spin-exotic signal with $J^{PC} = 1^{-+}$

Non resonant contributions

- Signal not necessarily from resonances
- Possible origin: Non-resonant contribution:
  - Same initial and final state
  - No intermediate 3π resonances appear

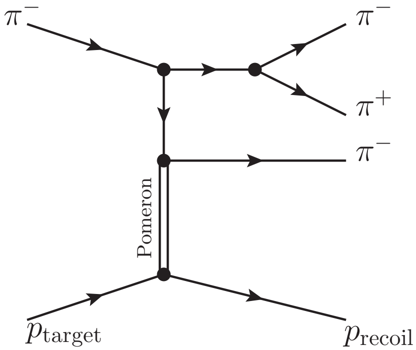

A spin-exotic signal with $J^{PC} = 1^{-+}$

Non resonant contributions

- Signal not necessarily from resonances
- Possible origin: Non-resonant contribution:
  - Same initial and final state
  - No intermediate 3π resonances appear
- Isobaric waves: Resonance assumed
- Effects on the Partial-Wave Analysis?

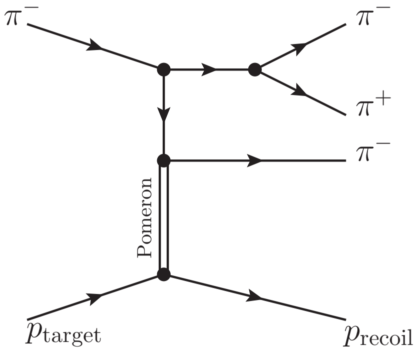

- Graph depicts the so-called Deck-effect
- Investigate influence on PWA:
  - Use simple model for this kind of process
  - Generate Monte Carlo data
  - Perform the same analysis on the MC data
  - Compare with results for real data

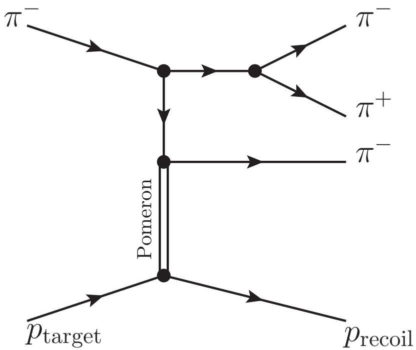

A spin-exotic signal with $J^{PC} = 1^{-+}$

Comparison with *Deck-model* at different t'-bins

- Low t': the intensities are very similar

$0.100 < t' < 0.113\,(\mathrm{GeV}/c)^2$

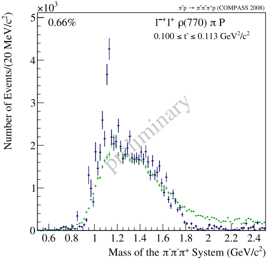

$0.164 < t' < 0.189\,(\mathrm{GeV}/c)^2$

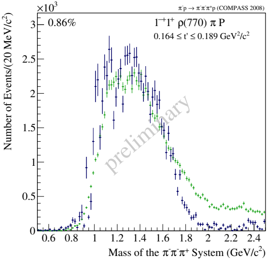

Result of the PWA and Deck-model scaled to integrated intensity

- Low t': the intensities are very similar
- High t': data exceeds non-resonant intensity

$0.100 < t' < 0.113\,(\mathrm{GeV}/c)^2$

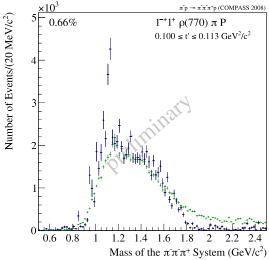

$0.326 < t' < 0.449\,(\mathrm{GeV}/c)^2$

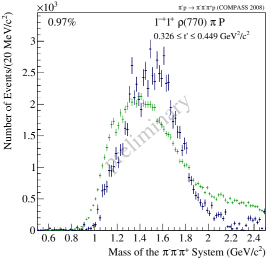

$0.164 < t' < 0.189\,(\mathrm{GeV}/c)^2$

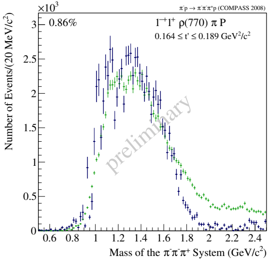

$0.724 < t' < 1.000\,(\mathrm{GeV}/c)^2$

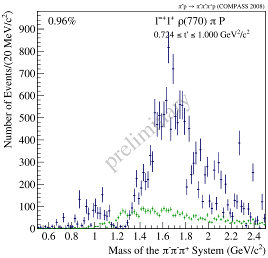

Result of the PWA and Deck-model scaled to integrated intensity

A spin-exotic signal with $J^{PC} = 1^{-+}$

Comparison with *Deck-model* at different t'-bins

- Low t': the intensities are very similar
- High t': data exceeds non-resonant intensity
- Resonance does not depend on t'

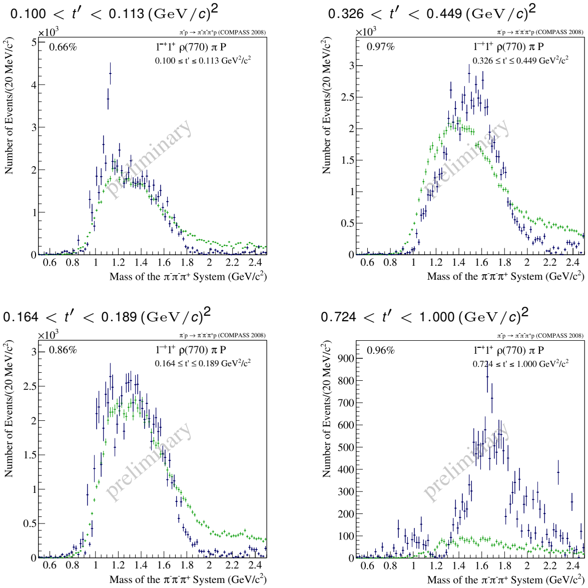

Result of the PWA and Deck-model scaled to integrated intensity

A spin-exotic signal with $J^{PC} = 1^{-+}$

Comparison with *Deck-model* at different t'-bins

- Low t': the intensities are very similar
- High t': data exceeds non-resonant intensity
- Resonance does not depend on t'
- Resonant contribution?

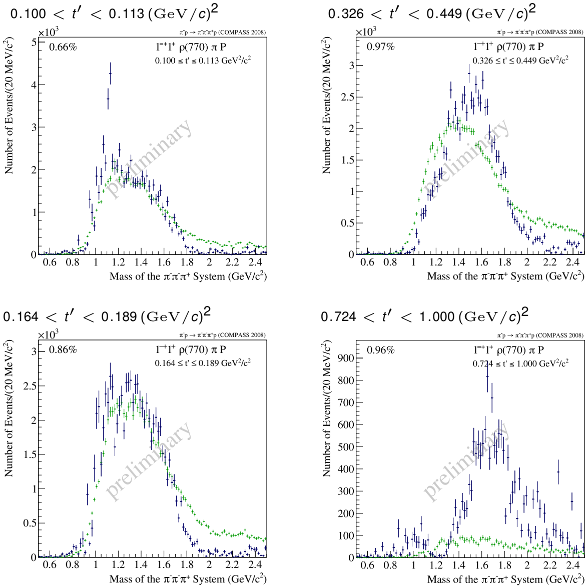

Result of the PWA and Deck-model scaled to integrated intensity

Inclusion of non-isobaric waves

- Already seen one non-isobaric contribution
- Monte-Carlo method not satisfying
- Non isobaric amplitude directly in first step:

$$\mathcal{A} = \sum_{\text{waves}} T_{\text{wave}}\mathcal{A}_{\text{wave}} + T_{\text{non}}\mathcal{A}_{\text{non}}$$

- T_{non} also free in the fit
- $\mathcal{A}_{\text{non}}$ projects to infinite number of Partial-Waves

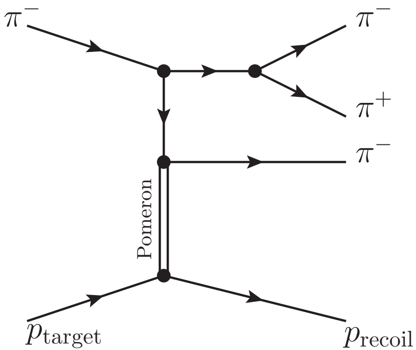

Non-isobaric waves

- Many possible processes
- Advantages:
  - Interference between isobaric and non-isobaric waves
  - $\mathcal{A}_{\text{non}}$ represents sum of infinite number of Partial-Waves
  - Less Partial-Waves necessary in the fit model
- Difficulties:
  - Non-isobaric amplitude affects all other waves
  - Strong model-dependence
  - $\rightarrow$ Determine first with kinematic fits
- Work in progress

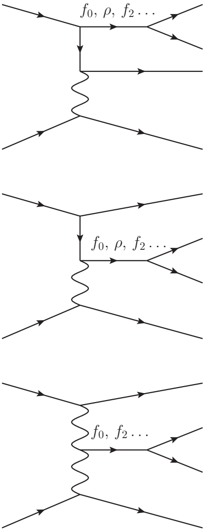

Extraction of the isobar structure
(*Freed-isobar approach*)

- Up to now: Parametrizations of isobars put into the fit beforehand

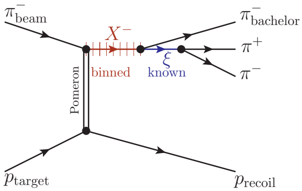

- Up to now: Parametrizations of isobars put into the fit beforehand
- Isobars:

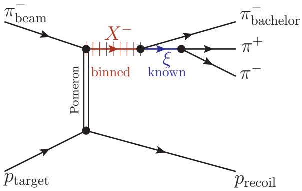

- Up to now: Parametrizations of isobars put into the fit beforehand
- Isobars:
  - $J^{PC} = 0^{++}$: $[\pi\pi]_S$,

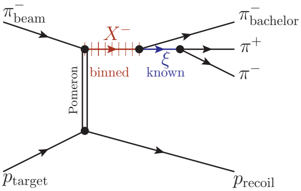

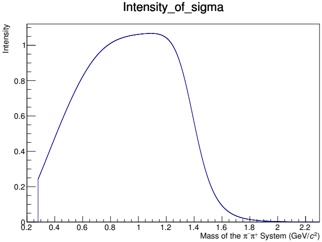

- Up to now: Parametrizations of isobars put into the fit beforehand
- Isobars:
  - $J^{PC} = 0^{++}$: $[\pi\pi]_S, f_0(980)$,

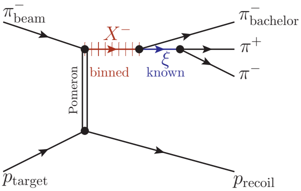

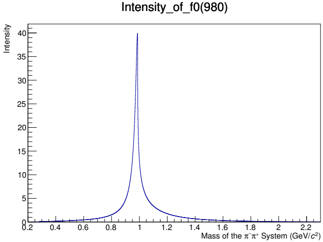

- Up to now: Parametrizations of isobars put into the fit beforehand
- Isobars:
  - $J^{PC} = 0^{++}$: $[\pi\pi]_S$, $f_0(980)$, $f_0(1500)$

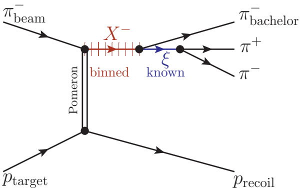

- Up to now: Parametrizations of isobars put into the fit beforehand
- Isobars:
  - $J^{PC} = 0^{++}$: $[\pi\pi]_S, f_0(980), f_0(1500)$
  - $J^{PC} = 1^{--}$: $\rho(770)$

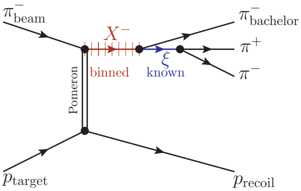

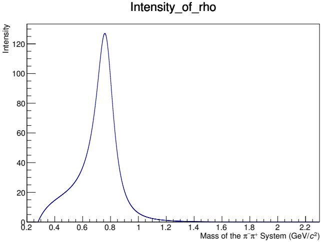

- Up to now: Parametrizations of isobars put into the fit beforehand
- Isobars:
  - $J^{PC} = 0^{++}$: $[\pi\pi]_S, f_0(980), f_0(1500)$
  - $J^{PC} = 1^{--}$: $\rho(770)$
  - $J^{PC} = 2^{++}$: $f_2(1270)$

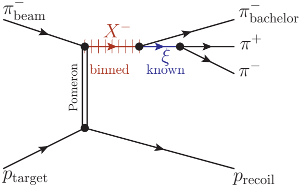

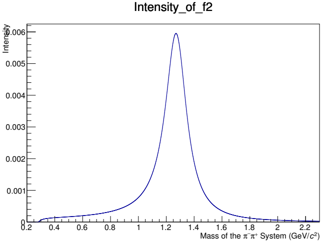

- Up to now: Parametrizations of isobars put into the fit beforehand
- Isobars:
  - $J^{PC} = 0^{++}$: $[\pi\pi]_S$, $f_0(980)$, $f_0(1500)$
  - $J^{PC} = 1^{--}$: $\rho(770)$
  - $J^{PC} = 2^{++}$: $f_2(1270)$
  - $J^{PC} = 3^{--}$: $\rho_3(1690)$

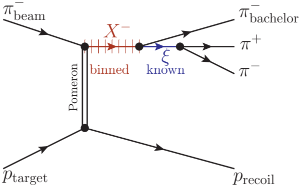

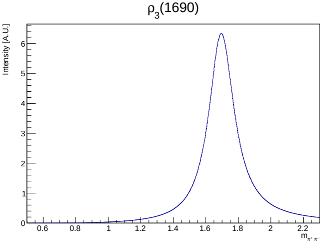

- Up to now: Parametrizations of isobars put into the fit beforehand
- Isobars:
  - $J^{PC} = 0^{++}$: $[\pi\pi]_S, f_0(980), f_0(1500)$
  - $J^{PC} = 1^{--}$: $\rho(770)$
  - $J^{PC} = 2^{++}$: $f_2(1270)$
  - $J^{PC} = 3^{--}$: $\rho_3(1690)$
- Parameterizations not perfect → Might distort the analysis

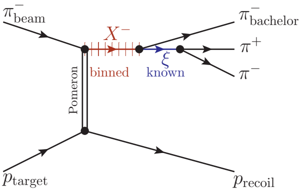

- Up to now: Parametrizations of isobars put into the fit beforehand
- Isobars:
  - $J^{PC} = 0^{++}$: $[\pi\pi]_S$, $f_0(980)$, $f_0(1500)$
  - $J^{PC} = 1^{--}$: $\rho(770)$
  - $J^{PC} = 2^{++}$: $f_2(1270)$
  - $J^{PC} = 3^{--}$: $\rho_3(1690)$
- Parameterizations not perfect → Might distort the analysis
- → Binned amplitudes instead of isobar parameterizations

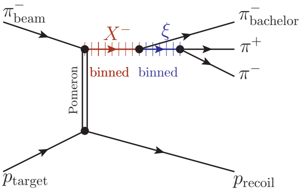

- Up to now: Complex shapes of isobars known beforehand

Intensity of 0^{++} isobars

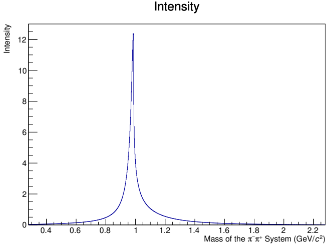

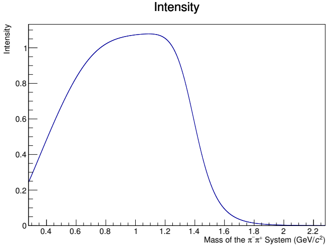

- Up to now: Complex shapes of isobars known beforehand
- May add up to complicated shape

Intensity of 0^{++} isobars

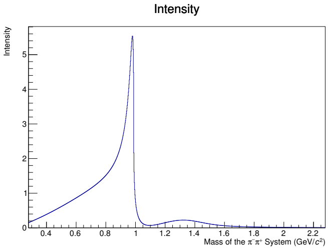

- Up to now: Complex shapes of isobars known beforehand
- May add up to complicated shape
- Now: Replaced by series of piecewise constant functions

Intensity of 0^{++} isobars

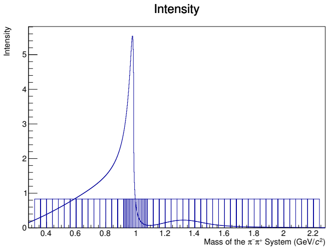

Freed-isobar approach

Basic idea

- Up to now: Complex shapes of isobars known beforehand
- May add up to complicated shape
- Now: Replaced by series of piecewise constant functions
- Binned amplitude of the isobars can be determined in the fit

Intensity of 0^{++} isobars

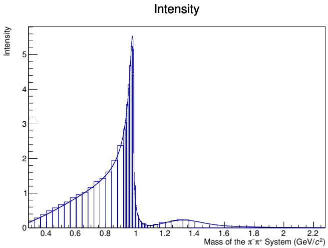

- Up to now: Complex shapes of isobars known beforehand
- May add up to complicated shape
- Now: Replaced by series of piecewise constant functions
- Binned amplitude of the isobars can be determined in the fit
- The set of binned functions is denoted as $[\pi\pi]_{0^{++}}$

Intensity of 0^{++} isobars

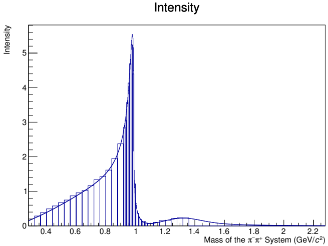

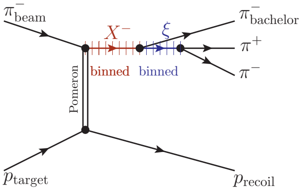

- Three waves with 0^{++} isobars freed:
  - $0^{-+}0^{+}[\pi\pi]_{0^{++}}\ \pi\ S$
  - $1^{++}0^{+}[\pi\pi]_{0^{++}}\ \pi\ P$
  - $2^{-+}0^{+}[\pi\pi]_{0^{++}}\ \pi\ D$
- Other 81 waves in the wave-set unchanged and fitted with fixed parametrizations
- Analysis done in bins of $m_{3\pi}$ $\rightarrow$ Two-dimensional picture

Two-dimensional intensities for the freed waves

MASS OF THE $\pi^-\pi^+$ SYSTEM

MASS OF THE $\pi^-\pi^+\pi^-$ SYSTEM

These plots should not be mistaken as Dalitz plots

Two-dimensional intensities for the freed waves

$0^{-+}0^{+}[\pi\pi]_{0^{++}}\ \pi\ S$

MASS OF THE $\pi^-\pi^+$ SYSTEM

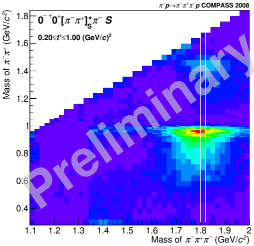

MASS OF THE $\pi^-\pi^+\pi^-$ SYSTEM

These plots should not be mistaken as Dalitz plots

Two-dimensional intensities for the freed waves

MASS OF THE $\pi^-\pi^+$ SYSTEM

$0^{-+}0^+[\pi\pi]_{0^{++}}\ \pi\ S$

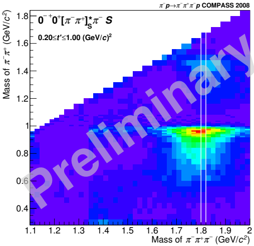

$1^{++}0^+[\pi\pi]_{0^{++}}\ \pi\ P$

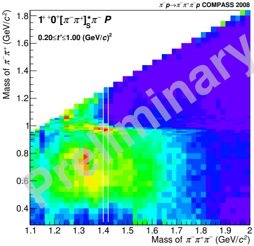

MASS OF THE $\pi^-\pi^+\pi^-$ SYSTEM

These plots should not be mistaken as Dalitz plots

Two-dimensional intensities for the freed waves

MASS OF THE $\pi^-\pi^+$ SYSTEM

$0^{-+}0^+[\pi\pi]_{0^{++}}\ \pi\ S$

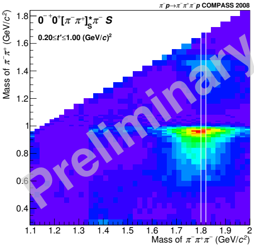

$1^{++}0^+[\pi\pi]_{0^{++}}\ \pi\ P$

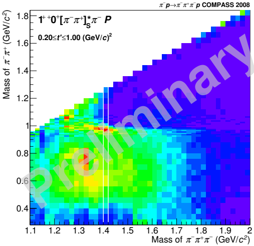

$2^{-+}0^+[\pi\pi]_{0^{++}}\ \pi\ D$

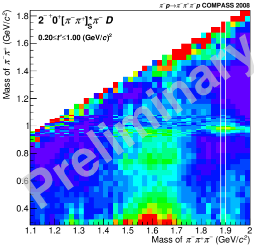

MASS OF THE $\pi^-\pi^+\pi^-$ SYSTEM

These plots should not be mistaken as Dalitz plots

Conclusions

- Huge data sets collected by COMPASS

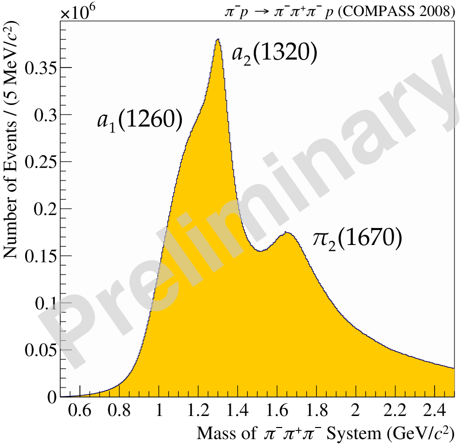

Conclusions

- Huge data sets collected by COMPASS
- Very detailed Partial-Wave Analysis

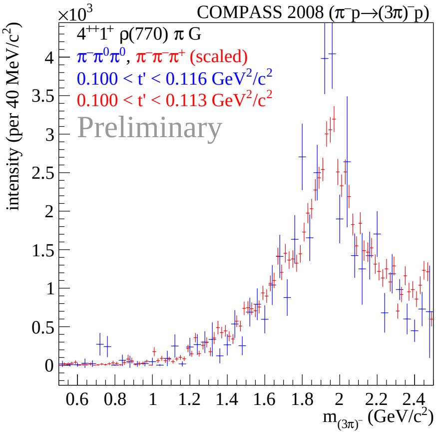

Conclusions

- Huge data sets collected by COMPASS
- Very detailed Partial-Wave Analysis
- Two-step fit-procedure

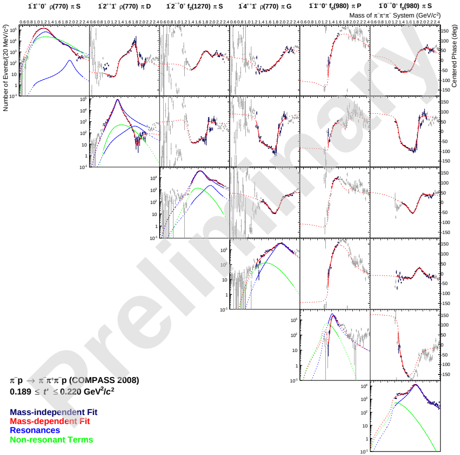

Conclusions

- Huge data sets collected by COMPASS
- Very detailed Partial-Wave Analysis
- Two-step fit-procedure
- New resonance signal

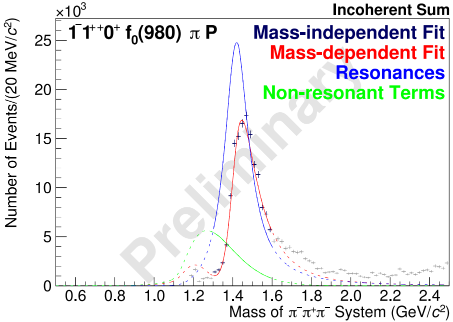

Conclusions

- Huge data sets collected by COMPASS
- Very detailed Partial-Wave Analysis
- Two-step fit-procedure
- New resonance signal
- Intensity in spin-exotic wave

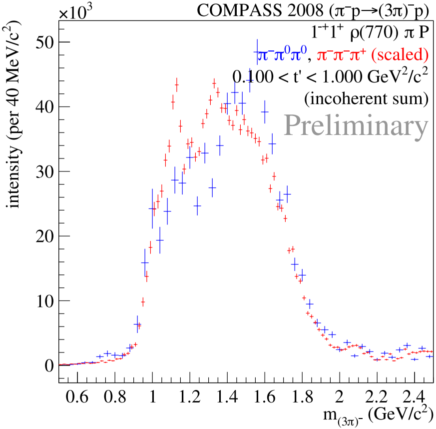

Conclusions

- Huge data sets collected by COMPASS
- Very detailed Partial-Wave Analysis
- Two-step fit-procedure
- New resonance signal
- Intensity in spin-exotic wave

Outlook

- Use new methods for wave-set selection

Not presented here

Conclusions

- Huge data sets collected by COMPASS
- Very detailed Partial-Wave Analysis
- Two-step fit-procedure
- New resonance signal
- Intensity in spin-exotic wave

Outlook

- Use new methods for wave-set selection
- Include non-resonant amplitudes

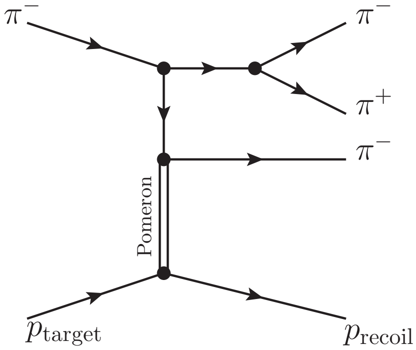

Conclusions

- Huge data sets collected by COMPASS
- Very detailed Partial-Wave Analysis
- Two-step fit-procedure
- New resonance signal
- Intensity in spin-exotic wave

Outlook

- Use new methods for wave-set selection
- Include non-resonant amplitudes
- Extract also isobar shapes